Electronic Supplementary Material (ESI) for Lab on a Chip.

Electronic Supplementary Information

Microdissected "cuboids" for microfluidic drug testing of intact tissues

Lisa F. Horowitz[a¥*], Adan D. Rodriguez[a*], Allan Au-Yeung[a,b], Kevin W. Bishop[a,c], Lindsey A. Barner[c], Gargi Mishra[d,f], Aashik Raman[a], Priscilla Delgado[a], Jonathan T.C. Liu[a,c,e], Taranjit S. Gujral[f], Mehdi Mehrabi[g], Mengsu Yang[b], Robert H. Pierce[d], and Albert Folch[a]

[a] Department of Bioengineering, University of Washington, Seattle, WA, USA

[b] Department of Biomedical Sciences, City University of Hong Kong, Hong Kong, China

[c] Department of Mechanical Engineering, University of Washington, Seattle, WA, USA

[d] Clinical Research Division, Fred Hutchinson Cancer Research Center, Seattle, WA, USA

[e] Department of Laboratory Medicine and Pathology, University of Washington, Seattle, WA, USA

[f] Human Biology Division, Fred Hutchinson Cancer Research Center, Seattle, WA, USA

[g] Department of Mechanical and Aeronautical Engineering, University of Pretoria, Pretoria, South Africa

Supplementary methods

Pressure drop in a trapezoidal microchannel

As reported by Takeuchi et.al., we applied the Darcy-Weisbach equation to approximate the resistance of the trapezoidal microchannels:

$$\Delta P = \frac{fL\rho V^2}{2D}$$

Equation 1 Darcy-Weisbach pressure drop equation

where f is the Darcy friction factor, L is the length of the channel, ρ is the fluid density, V is the average velocity of the fluid, and D is the hydraulic diameter, respectively[1,2]. D for a trapezoidal microchannel can be further expressed as

$$D = \frac{h(W_b + W_t)}{W_b + 2\sqrt{\frac{W_t - W_b}{2} + h^2}}$$

Equation 2 Hydraulic diameter of a trapezoidal microchannel

where h is the height and W_b and W_t are the bottom and top widths of the microchannel respectively. The Darcy friction factor, *f*, is related to the aspect ratio of the microchannels (W_b / W_t) and the Reynolds number:

$$Re = \frac{\rho V D}{\mu}$$

Equation 3 Reynold's number

where μ is the fluid viscosity. The following expression[3] has been widely used to predict the friction factor for fully developed laminar flow in rectangular microchannels of aspect ratio α (width / height):

$$fRe = 96(1 - 1.3553\alpha + 1.9467\alpha^2 - 1.7012\alpha^3 + 0.9564\alpha^4 - 0.2537\alpha^5)$$

Equation 4 Laminar friction constant equation for rectangular microchannels

Similarly, other groups have investigated a similar expression to estimate the friction constant for trapezoidal microchannels. Cheng et.al. experimentally obtained the following expression[4] to correlate

the laminar friction constant of trapezoidal microchannels in terms of the cross-sectional aspect ratio (W_b / W_t):

$$fRe = 11.43 + 0.80 \exp\left(\frac{2.67\ W_b}{W_t}\right)$$

Equation 5 Laminar friction constant estimation of trapezoidal microchannels

Since the traps in our microfluidic device have a rectangular shape, we had to utilize both expressions to estimate the pressure drop along path 1.

Suppl. Table 1. Hydraulic resistance ratios (RB/RT) after channel geometrical alterations

	1	**2**	**3**
Height Bypass	650 µm	650 µm	650 µm
Height Trap Channel	750 µm	800 µm	850 µm
RB/RT: Darcy-Weisbach	1.64	1.92	2.37

Supplementary figures

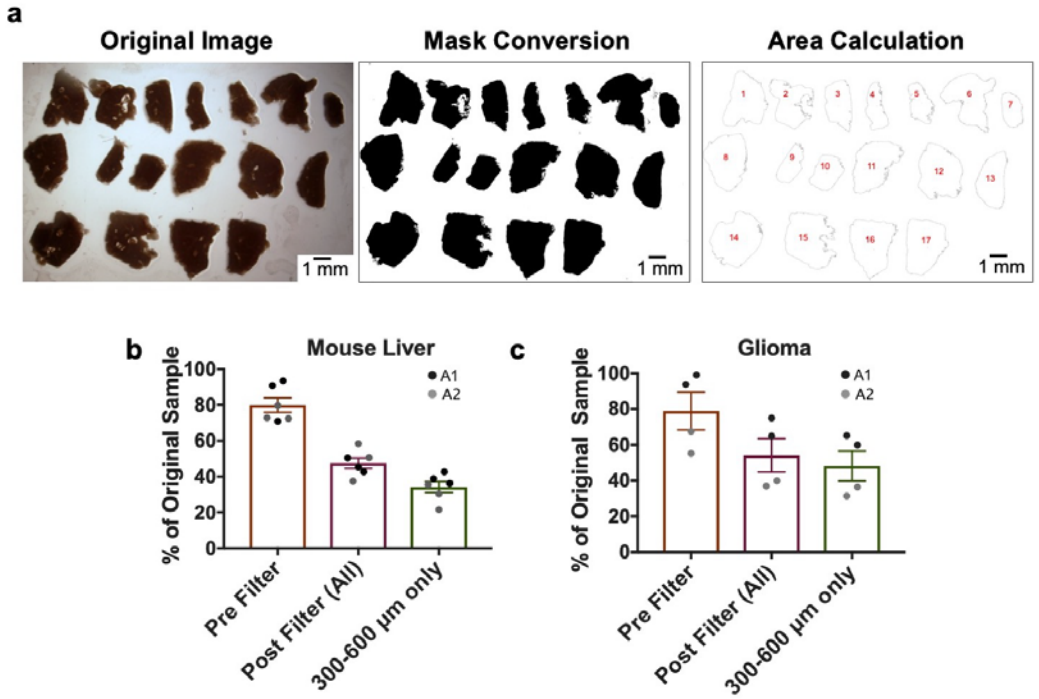

Suppl. Fig. 1. Sample yield analysis. (a) Image processing for total area calculation of slice samples (showing mouse liver slices). The % yield from the initial sample was estimated by taking the ratio of the total cuboid area after each step of the cuboid dissection process. Graphs show (b) mouse liver and (c) glioma cuboid sample yield pre- and post- filtering and the total area of cuboids between 300-600 µm. Individual points and ave ± s.e.m. N=6 for both mouse liver and glioma.

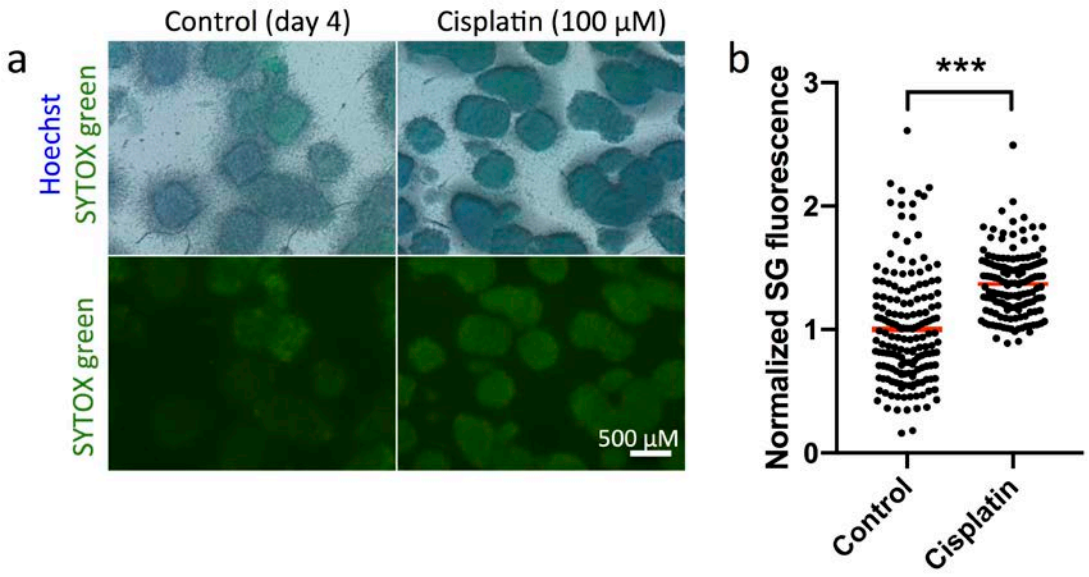

Suppl. Fig. 2. Cuboid drug treatment off-device. (a) Cuboids (no size filtering) after treatment with Cisplatin for 48 hours from day 2 to day 4 in culture. SYTOX green (SG) green nuclear stain and Hoechst blue nuclear stain overlayed on brightfield, or SG alone. (b) Graph of mean SG fluorescence normalized to average fluorescence of controls. Control (N=169) and cisplatin (N=145). Individual points and average. Student's T-test with Welch's correction. ***P<0.001

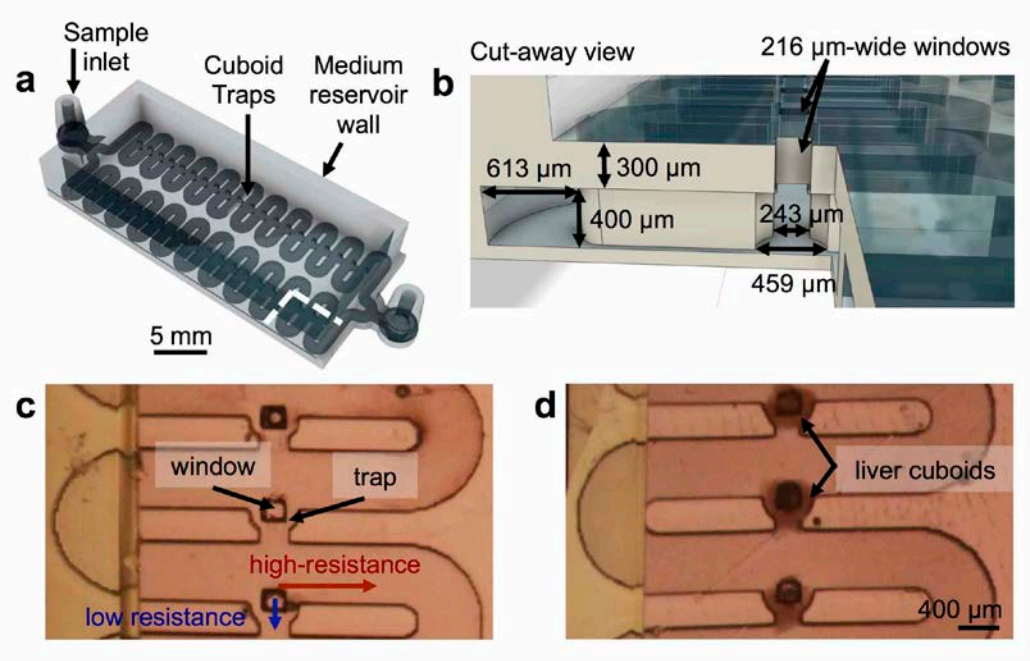

Suppl. Figure 3. 3D printed prototype of cuboid hydrodynamic trap array. (a) Oblique projection of the device rendered in Fusion 360. The initial straight channel bifurcates into two serpentine channels with cuboid traps, which then combine into a single outflow channel. Walls create a medium reservoir. (b) Cut-away close up view, with area removed demarcated in (a) by a white dotted line. The puncture-to-open wells have a thin window in the roof (not drawn). Once the cuboids are loaded, one can puncture the window with a needle to provide access of culture medium from the overlaying reservoir. (c) Top view of an empty region of the device, 3D printed using the Asiga Pico2 HD (pixels 27 µm x 27 µm, Z layer thickness 25 µm). The high and low flow resistance paths enable trapping. Once a cuboid is captured in trap, blocking flow through the trap, the next cuboid flows along for capture in the next trap. (d) Region after trapping of 400 µm fixed liver cuboids, subsequent application of collagen, and finally, placement of medium in the overlying reservoir.

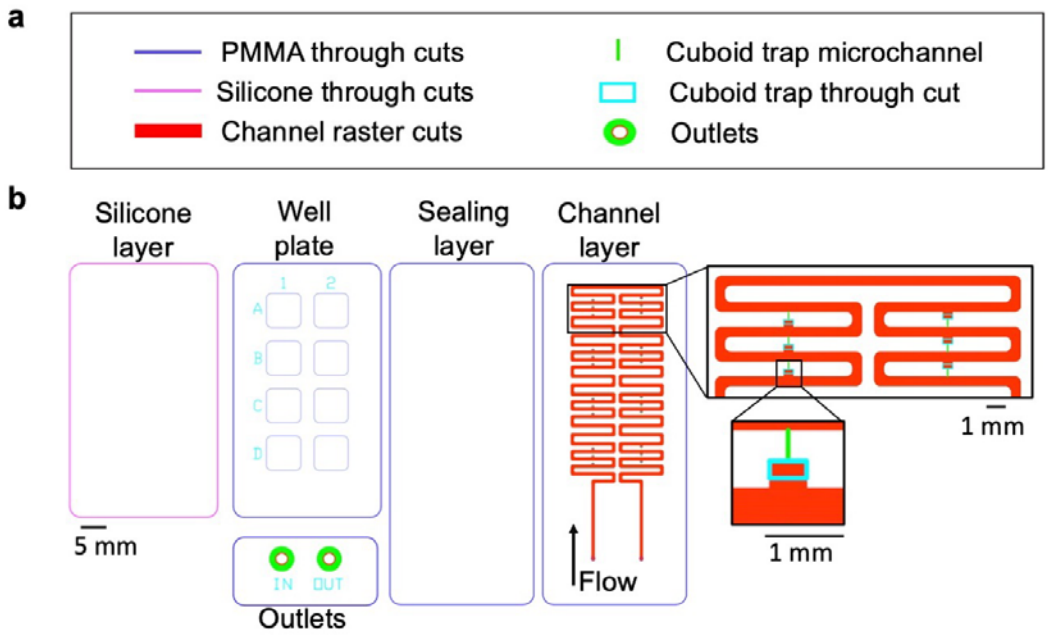

Suppl. Fig. 4. CAD Drawings. (a) Various laser-cutting elements used to make the microfluidic device layers. (b) CAD drawings showing the silicone adhesive layer, bottomless-well plate and outlets, sealing layer, and channel layer of the device with a magnification of the trapping areas.

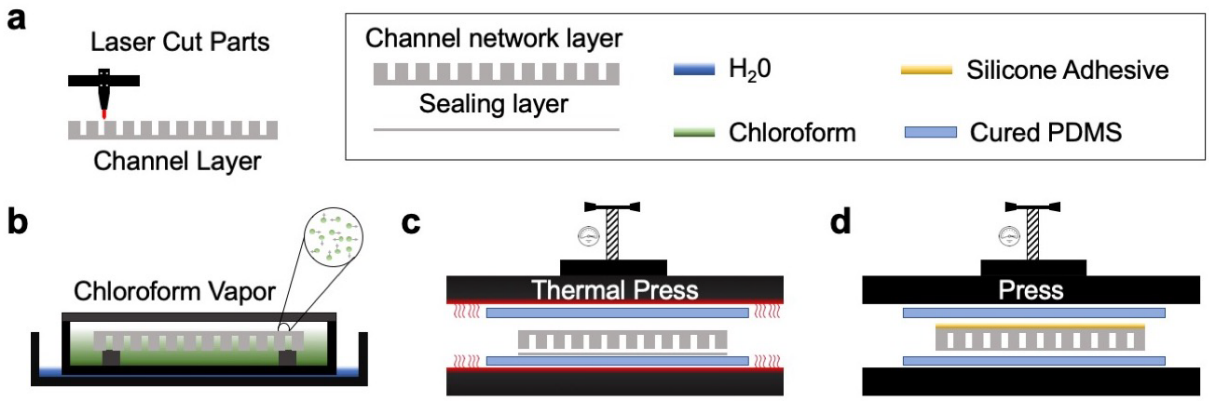

Suppl. Fig. 5. Fabrication process overview. General overview of device fabrication process. (a) Laser cutting/engraving and cleaning each of the laminates and components that compose the microfluidic device (10 min). (b) Chloroform vapor exposure (5 min). (c) Thermal press bonding (2 min). (d) Adhesive bonding of double sided polysil silicone adhesive (1 min). Final steps (not shown) are outlet installation and removal of silicone and attachment of bottomless 8-well plate.

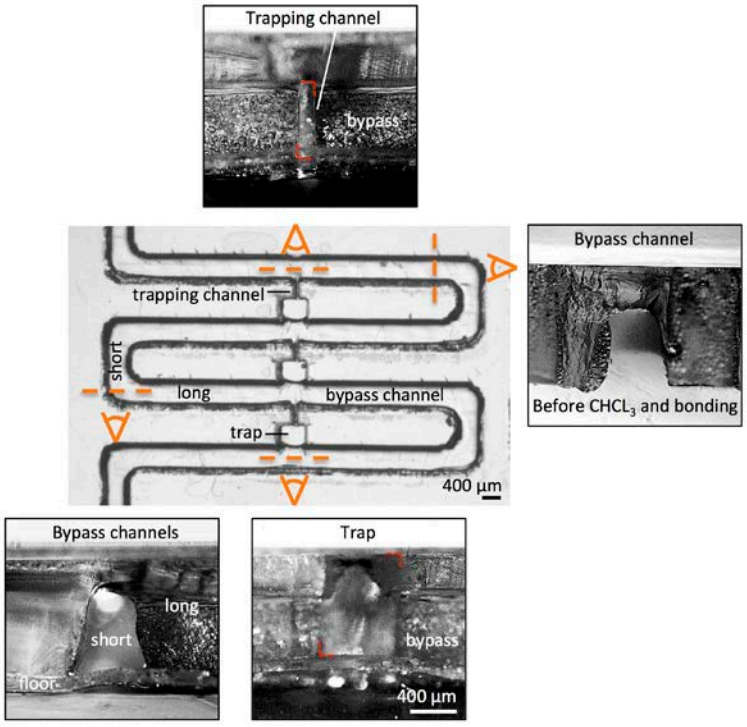

Suppl. Fig. 6. Microfluidic device geometry. Top-view and cross-sectional views of the device after making various breaks to expose the features. Representative locations of the breaks (dotted lines) and point-of-view (eye symbol) are shown. Cross-section of the long portion of the bypass is shown before chloroform ($CHCL_3$) treatment and bonding. Other cross-sections are shown after $CHCL_3$ treatment and bonding to the floor. Red brackets delineate feature borders for the trap channel and for the trap (transition to trap channel visible inside).

Supplementary references

1. Teshima, T., Ishihara, H., Iwai, K., Adachi, A. & Takeuchi, S. A dynamic microarray device for paired bead-based analysis. *Lab Chip* **10**, 2443 (2010).
2. Tan, W.-H. & Takeuchi, S. A trap-and-release integrated microfluidic system for dynamic microarray applications. *Proc. Natl. Acad. Sci.* **104**, 1146–1151 (2007).
3. Liu, D. & Garimella, S. V. Investigation of Liquid Flow in Microchannels. *J. Thermophys. HEAT Transf.* **18**,
4. Wu, H. Y. & Cheng, P. Friction factors in smooth trapezoidal silicon microchannels with different aspect ratios. doi:10.1016/S0017-9310(03)00106-6